White Paper

Fabrication of Solid-State Nanopores for Biomolecule Detection with ORION NanoFab

ZEISS

We make it visible.

Fabrication of Solid-State Nanopores for Biomolecule Detection with ORION NanoFab

Authors: Dr. Jijin Yang
Carl Zeiss Microscopy, LLC, USA
Dr. Adam Hall
Joint School of Nanoscience and Nanoengineering, University of North Carolina, USA

Date: August 2012

Background

Solid-state nanopores[1] are among a class of devices capable of biological detection at the single-molecule level. The technique involves monitoring the flow of ionic current through a fabricated aperture in a thin insulating membrane (usually low stress, amorphous silicon nitride, SiN), and detecting changes in this current as bio-molecules pass through. This technique has been used successfully to detect properties of various biomolecules including DNA[2, 3], RNA[4], proteins[5] and nucleoprotein filaments[6] and holds great potential for future genetic and epigenetic analysis schemes.

Challenge

Routine fabrication of nanopores or nanopore arrays with sub-5 nm features poses technical challenges. Procedures have been reported using a Focused Ion Beam (FIB)[8], an unfocused ion beam[2] and a Transmission Electron Microscope (TEM)[7], however limitations exist with each. For instance, the FIB method can only produce pores with a minimum diameter of 10-20 nm using a single, direct exposure, limiting the range of achievable dimensions and thus the potential applications of the devices. Both the unfocused ion beam and TEM methods allow much greater control over feature size, but at the expense of exposure time; minutes to hours are required to produce a single pore and only a single device can be loaded at a time. An ideal fabrication process should be able to generate reproducibly a wide range of nanopore sizes at high throughput and with low exposure time.

ORION NanoFab Solution

The Helium Ion Microscope (HIM) offers a fast, one-step process for fabricating solid-state nanopores using a helium ion beam with controllable current and a probe size of ca. 0.5 nm. For the samples presented here[9], the HIM beam current is set by adjusting spot control and He pressure to 5 pA through a 10 µm aperture. Directly prior to pore formation at each sample window, beam focus and stigmation are optimized at a nearby area of the substrate. Once corrected, the beam is blanked and the SiN window is moved into the beam path. Lithographically-defined exposure is performed with a set ion dose, ablating material and forming the nanopore(s).

Figure 1 shows an example of typical parameters used for patterning and a typical procedure follows:

1. In Type pull-down menu, choose “Bitmap – dwell map”
2. Load the pattern image in Bitmap file window
   a. Pattern image size is 512 x 512 pixels in this example
   b. Each pixel results in a single nanopore
3. Set the patterning parameters as follows
   a. Under Dose, ensure that the beam current is same as the blanker current, set “control” to ion per cm^2 and set “repeats” to 1
   b. Under Pixel Spacing, set “unit” to nm and both “horizontal” and “vertical” to 1
   c. Under Scanning, set “dwell time” to achieve the desired total dose
   d. Under Size and Location, set “lines” to 512, “pixels” to 512, and “pattern rect unit” to nm
   e. Manually set FOV (in microscope settings window) to .512 µm

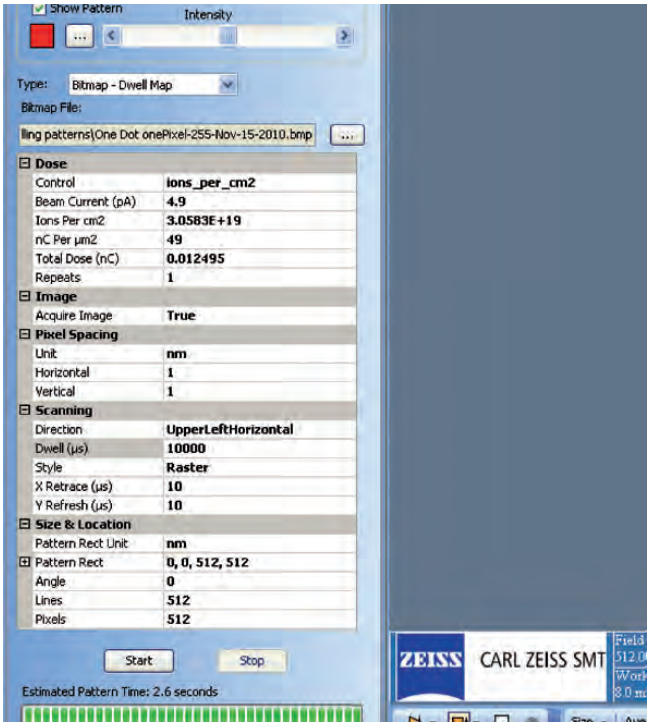

Figure 1

Screen shot of pattern parameters for nanopore milling.

After exposure, if desired, the resultant milled pattern can be imaged in-situ by HIM (Fig. 2a) using a transmission stage, where secondary electrons are instead recorded from a metal surface below the thin SiN window. The presence of an opening in the membrane results in a larger number of transmitted ions and thus greater secondary electron emission, creating a bright spot in the image. The lithographic nature of the process allows large area arrays to be made quickly while retaining the range of attainable nanopore diameters (Fig. 2a).

For a helium beam of constant current, the time of HIM exposure can be used to control the ion dose and correspondingly the diameter of the resultant nanopore. Fig. 2b shows a TEM image of nanopores fabricated with various exposure times. In each case, the opening is clear in the image. From these images, the area of the pore opening can be used to calculate the average diameter, which is found to correlate tightly (±3 nm on average) with ion dose (Fig. 2c). The doses shown correspond to exposure times from tens of milliseconds to about 12 seconds. From this relation, nanopores of any desired diameter can be produced controllably by adjusting the dose accordingly. The smallest diameter achieved under 5 pA current conditions is 3.7 nm (Fig. 2c inset). Large-diameter pores can be produced with equal ease by lithographically defining narrow ring-like patterns of any desired size (Fig. 3). Use of the ring pattern greatly reduces milling time and increases the upper limit on the sizes attainable with HIM into the range accessible by other common fabrication processes like photolithography or FIB. Furthermore, the 50 mm travel of the X-Y sample stage will allow numerous (100 or more) individual SiN window chips to be loaded simultaneously. This greatly increases the throughput of the HIM process over competing methods.

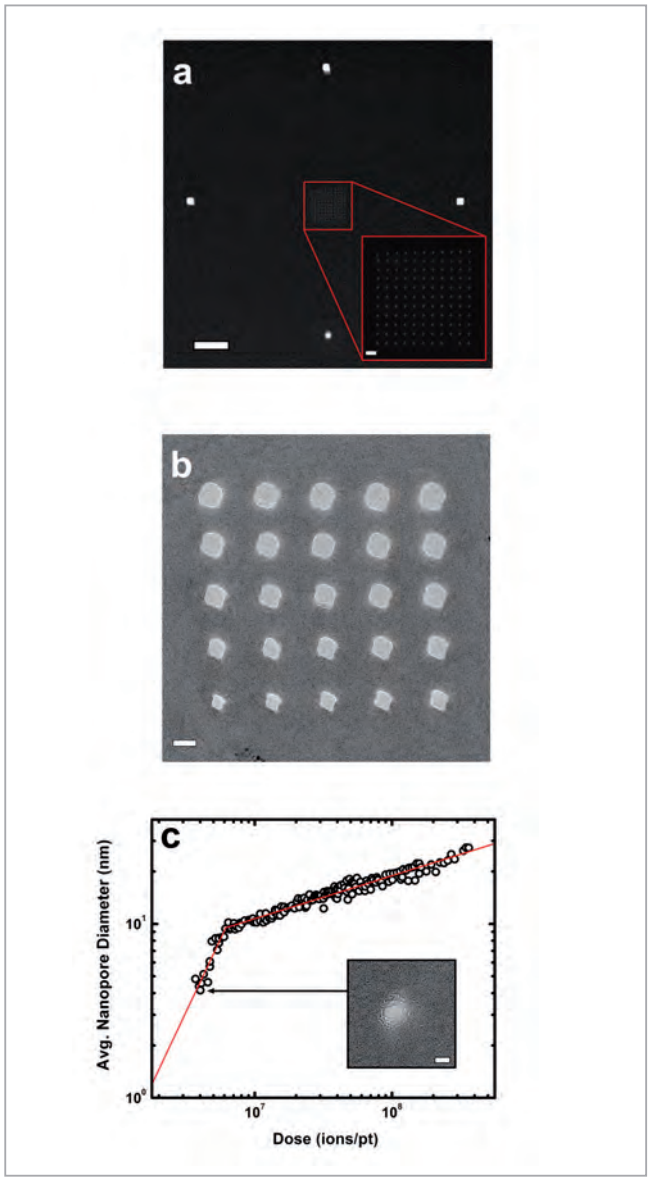

Figure 2

HIM Nanopore Formation

(a) Transmission mode HIM image of an 11 x 11 array of 5 nm diameter nanopores (total exposure time approximately 1 min) surrounded by four patterns of ca. 100 nm dimensions each. Scale bar represents 500 nm. Inset: A magnified view of the central nanopore array (scale bar is 50 nm). (b) Transmission electron micrograph of a HIM nanopore array in a 43 nm thick SiN membrane, formed with doses ranging from ca. 2800 (lower left) to ca. 47000 (upper right) ions/pt. Scale bar represents 20 nm. (c) Log-log plot of helium ion dose vs. resultant nanopore diameter, showing a high level of controllability. Inset shows a TEM image of the smallest pore yet produced with this method (3.7 nm). Scale bar represents 5 nm.

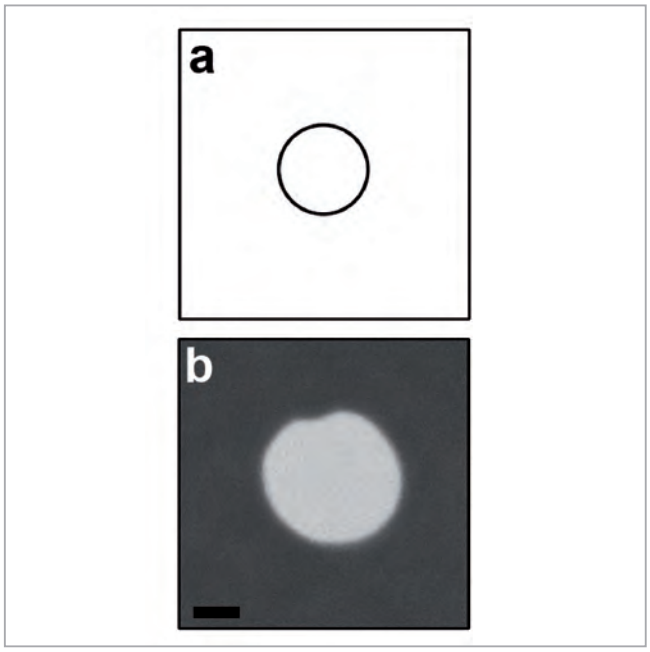

Figure 3

Large-diameter nanopore definition

(a) Ring-like lithographic pattern of defined size 100 nm. (b) Resultant large-diameter nanopore (120 nm).

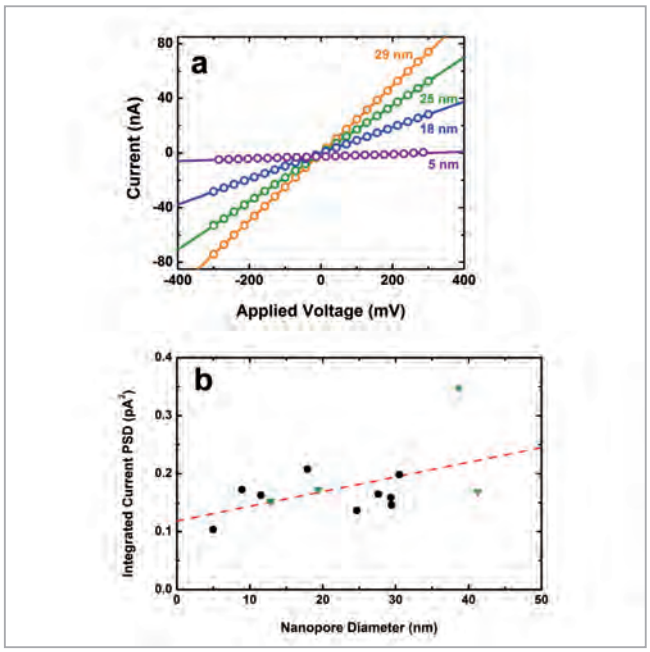

Figure 4

Ionic current noise analysis

(a) Linear I-V characteristics of HIM nanopores with diameters indicated. (b) Comparison of the integrated current power spectral density for HIM nanopores (green triangles) and TEM nanopores (black circles) of various diameter, showing the same trend. The red line is a linear fit to all points and is intended as a guide to the eye.

Biological detection

A SiN window chip containing a single nanopore can be loaded into a flow cell and introduced with an electrolyte solution (1 M KCl, 10 mM tris-HCl (pH 8.0), 1 mM EDTA) to allow ionic current measurements. It is found that nanopores formed with the HIM method exhibit linear I-V curves (Fig. 4a), as has been demonstrated with other methods. The ionic current noise level of HIM nanopores compares favorably with other methods as well. Fig. 4b shows the integrated current power spectral density (cumulative cross-spectral noise level) for several devices made with either HIM or with the standard TEM technique. This shows that the noise associated with HIM nanopores is comparable to that of TEM nanopores and will thus allow for similar detection capabilities.

As an example of these capabilities, double strand (ds) DNA translocations through a 25 nm nanopore are measured. λ dsDNA (48.5 kb) is loaded onto one side of the nanopore and a trans-membrane voltage is applied (Fig. 5a). This results in a series of downward spikes in the measured nanopore conductance (Fig. 5b), characteristic of dsDNA translocations. A histogram of all conductance data points (Fig. 6a) shows that the measured conductance levels fall into easily separable populations. Closer inspection (Fig. 6b) reveals structure within these events that is caused by different folding conformations of the molecule during translocation. The HIM nanopore used in this example is sufficiently stable to perform this measurement over a large range of applied voltage (100-800 mV), resulting in a total of over 9000 individual recorded events.

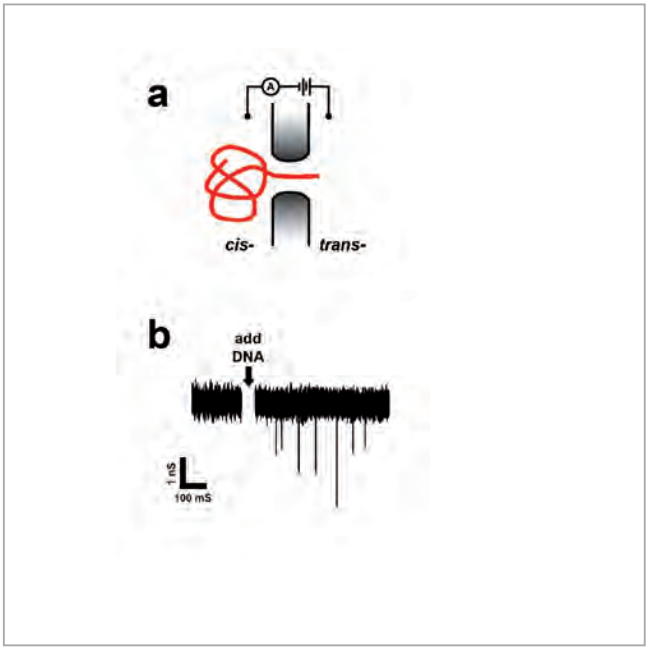

Figure 5
DNA detection with a HIM nanopore
(a) Schematic representation of the DNA translocation measurement.
(b) A typical measured conductance trace (V_{app} = 200 mV, low pass filtered at 10 kHz) revealing downward spikes after the addition of dsDNA.

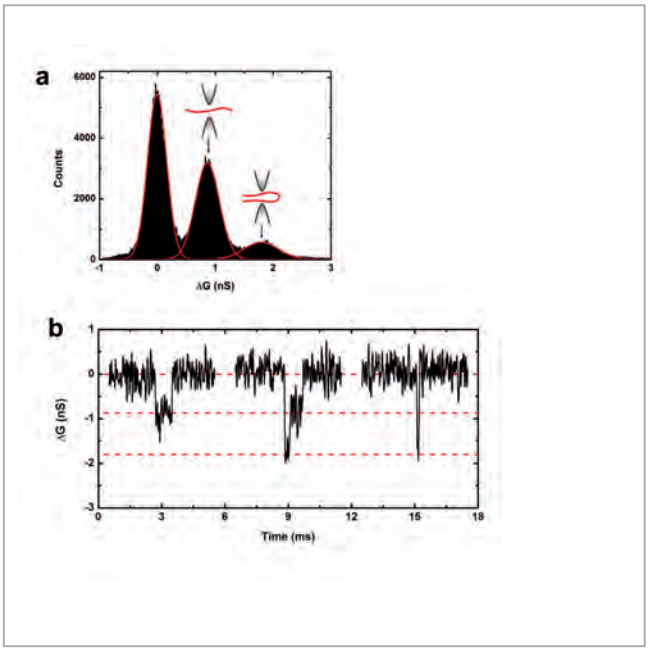

Figure 6
DNA translocation
(a) A histogram of all measured conductance points for 878 individual events. Insets show diagrammatic explanation of the adjacent peaks.
(b) Examples of individual events (V_{app} = 200 mV, low pass filtered at 10 kHz), indicating the translocation of unfolded (left), partially folded (center) and folded dsDNA (right). Red dashed lines represent the centers of the Gaussian fits from (a).

In summary, we have demonstrated the controlled fabrication of solid-state nanopores in thin SiN membranes using a scanning helium ion microscope. The method is remarkably fast and highly repeatable, and can achieve diameters as low as 4 nm reliably. We showed that nanopores formed with this method are capable of ionic transport and that the current noise properties are comparable to those of pores fabricated with a TEM. Finally, we demonstrated the efficacy of HIM nanopores in biomolecule detection experiments by performing dsDNA translocations.

Acknowledgment

We thank Colin Sanford, Dave Ferranti, Larry Scipioni and Lewis Stern for helpful discussions and comments.

Selected References:

[1] C. Dekker, Nat. Nanotech. 2 (4), 209-215 (2007).
[2] J. L. Li, M. Gershow, D. Stein, E. Brandin and J. A. Golovchenko, Nature Materials 2 (9), 611-615 (2003).
[3] A. J. Storm, J. H. Chen, H. W. Zandbergen and C. Dekker, Phys Rev E Stat Nonlin Soft Matter Phys 71 (5 Pt 1), 051903 (2005).
[4] G. M. Skinner, M. van den Hout, O. Broekmans, C. Dekker and N. H. Dekker, Nano Lett. 9 (8), 2953-2960 (2009).
[5] M. Firnkes, D. Pedone, J. Knezevic, M. Doblinger and U. Rant, Nano Lett. 10 (6), 2162-2167 (2010).
[6] R. M. M. Smeets, S. W. Kowalczyk, A. R. Hall, N. H. Dekker and C. Dekker, Nano Lett. 9 (9), 3089-3095 (2009).
[7] A. J. Storm, J. H. Chen, X. S. Ling, H. W. Zandbergen and C. Dekker, Nature Materials 2 (8), 537-540 (2003).
[8] A. A. Tseng, Small 1 (10), 924-939 (2005).
[9] J. Yang, D. C. Ferranti, L. A. Stern, C. A. Sanford, J. Huang, Z. Ren, L.-C. Qin and A. R. Hall, Nanotechnology, 22 (28), 285310 (2011)


facebook.com/zeissmicroscopy


twitter.com/zeiss_micro


youtube.com/zeissmicroscopy


flickr.com/zeissmicro

Carl Zeiss Microscopy GmbH
07745 Jena, Germany
microscopy@zeiss.com
www.zeiss.com/microscopy

We make it visible.